ELSEVIER

Journal of Physics and Chemistry of Solids 64 (2003) 385–390

JOURNAL OF PHYSICS AND CHEMISTRY OF SOLIDS

www.elsevier.com/locate/jpcs

Synthesis and characterization of Ni magnetic nanoparticles in AlMCM41 host

Jin-Seung Jung[a,*], Kyong-Hoon Choi[a], Weon-Sik Chae[b], Yong-Rok Kim[b], Jong-Ho Jun[c], Leszek Malkinski[d], Thomas Kodenkandath[e], Weilie Zhou[e], John B. Wiley[e], Charles J. O'Connor[e,*]

[a]*Department of Chemistry, Kangnung National University, Kangnung 210-702, South Korea*
[b]*Department of Chemistry, Yonsei University, Seoul 120-749, South Korea*
[c]*Department of Applied Chemistry, Konkuk University, Chungju 380-701, South Korea*
[d]*Institute of Physics, Polish Academy of Sciences, Warsaw, Poland*
[e]*Advanced Material Research Institute, University of New Orleans, New Orleans, LA 70148, USA*

Received 19 February 2002; accepted 25 March 2002

Abstract

Superparamagnetic nickel nanoparticles were prepared by incorporating nickel ion into AlMCM41 as a nanoreactor and then reduced with sodium borohydride or H_2 gas. Products were characterized by elemental analysis, transmission electron microscopy, X-ray powder diffraction, and magnetic susceptibility. The nickel particle size and blocking temperature depend on the reduction method.

Keywords: A. Nickel nanoparticles; A. MCM41; C. Transmission electron microscopy; C. X-ray diffraction; D. Magnetic properties

1. Introduction

The synthesis of non-agglomerated magnetic nanoparticles has attracted a great deal of attention for their interesting chemical and physical properties and potential technological applications [1–3]. The preparation of nanoscale magnetic materials with desired properties is difficult and the preparation of magnetic transition metal nanoparticles including nickel, cobalt, and iron presents a significant challenge. Such synthetic studies are often hindered by the spontaneous production of macroscopic-sized agglomerates which do not show the unique properties of independent nanoscale particles. The fabrication of agglomerated particles was made by sonochemical preparation techniques and the use of an inorganic matrix as a host for nanocrystalline particles [4–7].

Our objective is to develop nanosized magnetic particles in a non-magnetic matrix that induces better isolation and corrosion-resistant properties compared to their pure metal counterparts. Crystalline zeolites have widely been used as a stabilizing matrix for the preparation of highly dispersed metal particles, but they are limited to the pore size of less than 1 nm. The MCM41 materials possess a hexagonal arrangement of uniformly sized mesopores, which were first reported in 1992 [8]. Such narrow distribution of the controlled pore size in the mesoporous solids has been investigated for the use of nanometre-sized hosts in organizing guest metal clusters, metal oxides, semiconductor clusters, and conduction polymers, as well as catalysts in the refining industry [9,10]. In a recent report, we have described Ni nanoparticles in AlMCM41 which can be obtained during the sodium borohydride reduction of Ni^{2+}–AlMCM41 in aqueous solution [11]. As a part of our continuing efforts to understand and to control the formation of nanoscaled magnetic materials, we have studied the reduction of Ni^{2+} in the solid state. The advantage of this method lies

* Corresponding authors. Tel.: +82-33-640-2305; fax: +82-33-640-2738 (J.-S. Jung), Tel.: +1-504-280-6840; fax: +1-504-280-3185 (C.J. O'Connor).
E-mail addresses: jjscm@kangnung.ac.kr (J.-S. Jung), coconnor@uno.edu (C.J. O'Connor).

0022-3697/03/$ - see front matter © 2002 Elsevier Science Ltd. All rights reserved.
PII: S0022-3697(02)00279-2

Table 1
Energy dispersive X-ray spectroscopic profile and elemental analysis

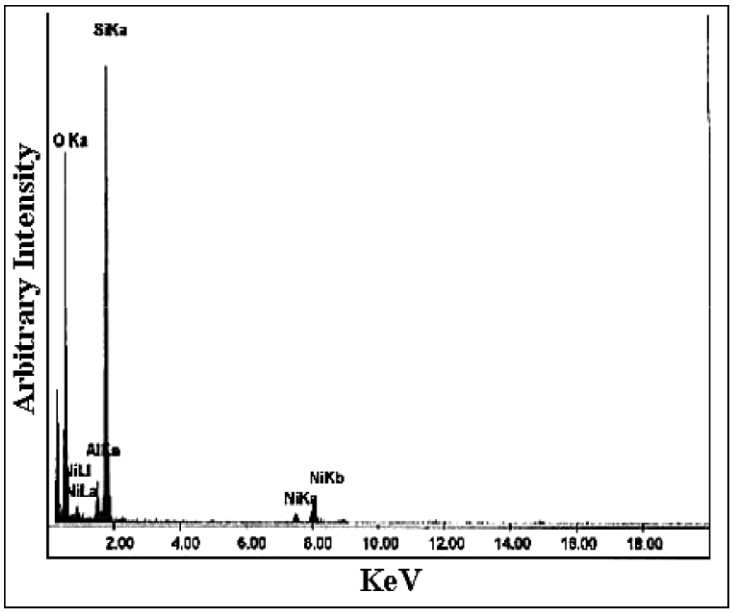

Element	Weight %	Atomic %
O K	51.9	65.8
AlK	3.2	2.4
SiK	43.3	31.3
NiK	1.6	0.5
Total	100.0	100.0

in the absence of the possible contaminants linked to the use of reductants [12]. Here we describe these experiments and how simple modification of the conditions leads to different magnetic properties.

2. Experimental

2.1. Synthesis

Ni^{2+}–AlMCM41 was prepared by the previously reported method [11]. AlMCM41 (0.2 g) was slowly stirred in 30 ml of 0.05 M $NiBr_2$ aqueous solution. The sample was then filtered and washed with distilled and deionized water. To maximize the extent of exchange, the ion exchange step was repeated five times. In order to remove the extrapore Ni^{2+} particles from the AlMCM41 host material, the resulting green powder of Ni^{2+}–AlMCM41 was suspended in distilled water for 1 h. Two different methods have been tried to reduce Ni^{2+} to Ni metal in AlMCM41 mesoporous materials. One is the liquid state Ni^{2+} ion reduction which is performed by the dropwise addition of $NaBH_4$ solution with stirring into 20 ml distilled water containing the Ni^{2+}–AlMCM41 powder and the other is the solid state reduction of Ni–AlMCM41 which is prepared from exposure to H_2–N_2 (4/96%, v/v) gas mixture at 450 °C for 3 h [13].

2.2. X-ray diffraction

X-ray powder diffraction (XRD) data were collected on a Philips X-Pert MPD system equipped with copper radiation ($2\theta = 1.5418$ Å) and a graphite monochrometer.

2.3. Transmission electron microscopy (TEM)

Samples were ultrasonically dispersed in acetone and a drop of the suspension was deposited on a carbon copper grid. Micrographs were taken on a JEOL 2010 microscope operated at 200 kV.

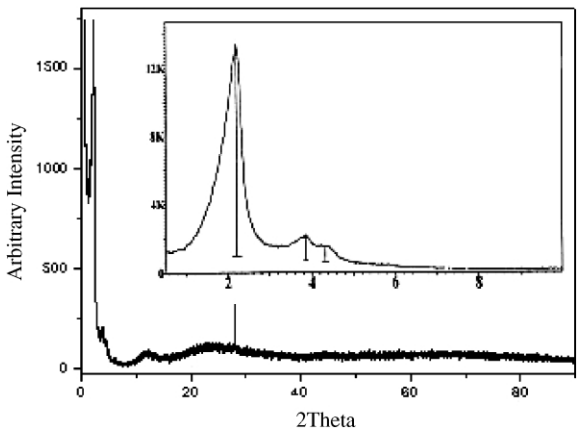

Fig. 1. XRD pattern of Ni–AlMCM41 prepared by H_2 reduction at 450 °C. Inset: XRD pattern of AlMCM41 host.

2.4. Magnetic measurements

The magnetic properties of the Ni–AlMCM41 were characterized using a Quantum Design Model MPMS-5S SQUID susceptometer. Calibration and measurement procedures have been described in detail elsewhere [14]. Two types of magnetic measurements were conducted: dc magnetic susceptibility as a function of temperature down to 1.7 K for both field-cooled (FC) and zero-field-cooled (ZFC) samples, and the magnetization measured as a function of magnetic field (hysteresis loops).

3. Results and discussion

The overall ion-exchange capacity in AlMCM41 is substantially higher than that in siliceous MCM41 since the ion exchange capacity depends on the net negative charge of the framework and not on the silanol group content in the host [15,16]. The incorporation of aluminum into the MCM framework induces a net negative charge in the framework and it is compensated by sodium cations. AlMCM41 host materials which are utilized in this experiment have the Si/Al ratio of 14. To get maximum Ni content in the host, it is necessary to have the highest possible Si/Al ratio. However, too high a ratio of the aluminum incorporation into MCM41 host causes the loss of the structural ordering [15].

Elemental analysis for Ni is determined to be 1.6 wt% in the Ni–AlMCM41 (Table 1). The extent of the ion exchange is not significantly different compared to the previous report [11]. Since AlMCM41 does not have the strict crystallographic order in an atomic scale, its wall structure cannot be determined from crystallographic data. However, the powder X-ray diffraction (XRD) pattern of AlMCM41 shows several low-index peaks, which reflect the quasi-regular arrangement of the mesopores with hexagonal symmetry [17]. In Fig. 1, we present XRD patterns of Ni–AlMCM41 prepared by hydrogen reduction at 450 °C.

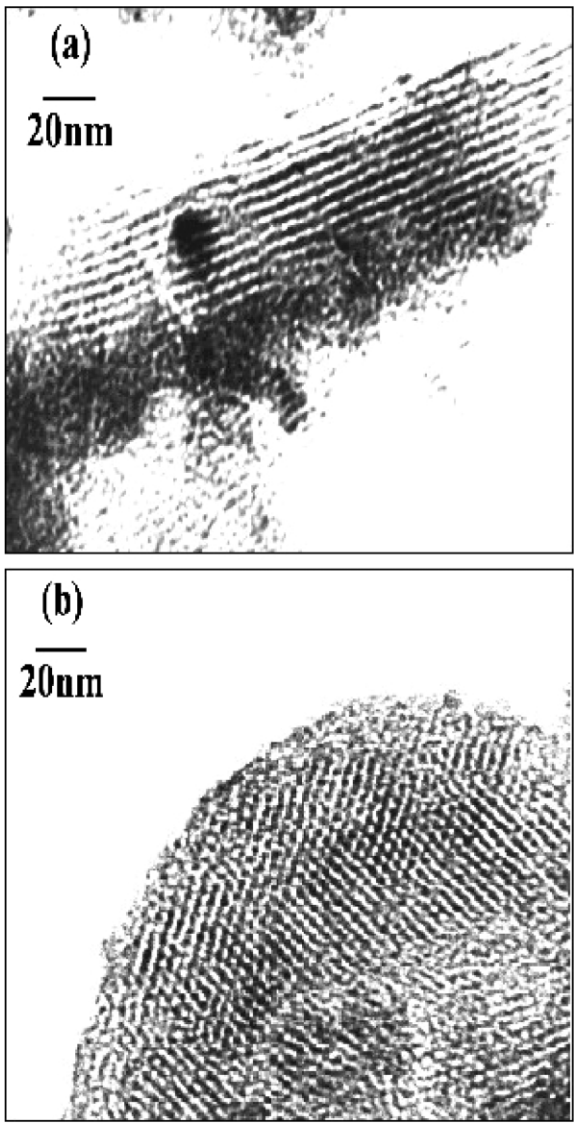

Fig. 2. Transmission electron micrographs of Ni–AlMCM41: (a) lamellar structure from the projection of a hexagonal array of tubules, (b) hexagonal pore structure.

The XRD pattern of the AlMCM41 host at low angle illustrates that the host material retains its regular pore structure even after the reduction at 450 °C. A direct and precise measurement of the host is highly desirable with respect to the characterization of this inclusion method. Such data were compared with the TEM images of Ni–AlMCM41 as well. In Fig. 2, two different TEM images are shown: (a) lamellar structure and (b) honeycomb structure, depending on the orientation of particles with respect to the electron beam direction [18]. The estimated interplanar

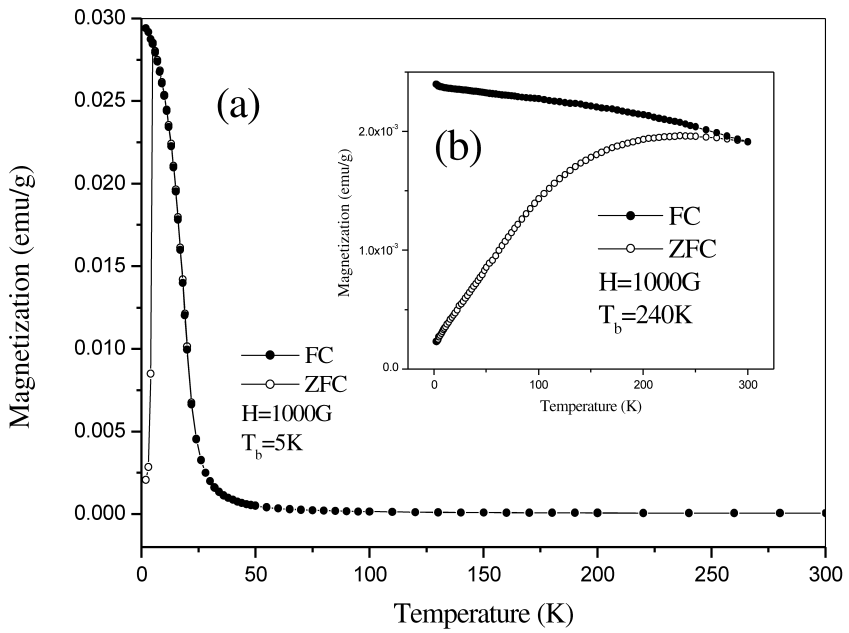

Fig. 3. Temperature dependent field-cooled and zero-field-cooled dc magnetic susceptibilities of Ni–AlMCM41. The samples were prepared by (a) solution reduction ($NaBH_4$) and (b) solid reduction (H_2) (inset).

distance in the lamellar structure is about 4.0 nm. It is well consistent with the XRD value ($2\theta = 2.2$).

Since elemental distributions of the microscopic region were of great concern with respect to TEM, the microscopic elemental composition analysis was obtained with energy dispersive X-ray spectroscopy (EDX). This result suggests that nickel particles are located within the AlMCM41 walls. Although EDX data clearly identify Ni in the AlMCM41 network, we were not able to isolate the image of single nickel nanoparticle in our TEM image due to the insufficient contrast between the pore spaces and the Ni particles. In this study, we demonstrate for the first time that Ni nanoparticles can be stabilized in AlMCM41 host with the conventional ion-exchange route which induces the exchange with $NiBr_2$ and the consequent reduction with hydrogen gas.

FC and ZFC magnetization experiments at low fields are very useful for the characterization of superparamagnetic properties [19]. As shown in Fig. 3, Ni nanoparticles obtained by two different reduction methods appear to have superparamagnetic properties in significantly different temperature ranges determined by characteristic temperatures, called blocking temperatures (T_b) [$T_b = 5$ K (solution method), $T_b = 240$ K (solid method)]. The maximum at around 5 K in the ZFC data for the sample prepared by the solution method, corresponds to the superparamagnetic blocking temperature (T_b), and indicates a very sharp and superimposed pattern without any deviation between ZFC and FC magnetic data at temperatures $T > T_b$ (Fig. 3). Also, the magnetization curves in the superparamagnetic state ($T > T_b$) should be unhysterectic (compare curves in Figs. 4 and 5). This data implies that the Ni clusters in AlMCM41 are uniformly distributed in their sizes and do not experience energetic couplings among them [20]. The Ni particle size is estimated to be 4.3 nm diameter from the blocking temperature which is defined as $T_B = KV/25k_B$ [21]. The paramagnetic Curie temperature is close to 0 K, which also means that the particles do not interact with each other. Another evidence for superparamagnetic properties of Ni particles is the Langevin shape of magnetization curves above blocking temperature. An example of Langevin function fitting to the experimental data measured at 20 K is presented in Fig. 6. The weight and volume fractions of Ni particles embedded in the host materials, which are necessary for renormalization of the data, were found by comparing the saturation magnetization measured at 2 K (Figs. 4 and 5) with the bulk magnetization of Ni. The volume of a single Ni particle V can be evaluated as m/M ratio from the fitting parameters M and $p = m/(Tk_B)$ presented in Fig. 6. The particle diameter calculated from the fitting parameters was about 1.9 nm. The size of particles prepared by the solid reduction method is estimated to be around 25 nm from the observed blocking temperature of 240 K. On the other hand, the fitting of the Langevin function to the data at 300 K results in a particle diameter of 14 nm, which is smaller than the one (25 nm) estimated from the blocking temperature. Since the extrapolated reciprocal susceptibility curve crosses the temperature axis at a positive value, interactions among the particles may shift the blocking temperature towards a higher temperature and, consequently, the size is over-estimated. It is also possible that the discrepancy between particle sizes evaluated from the blocking temperature and

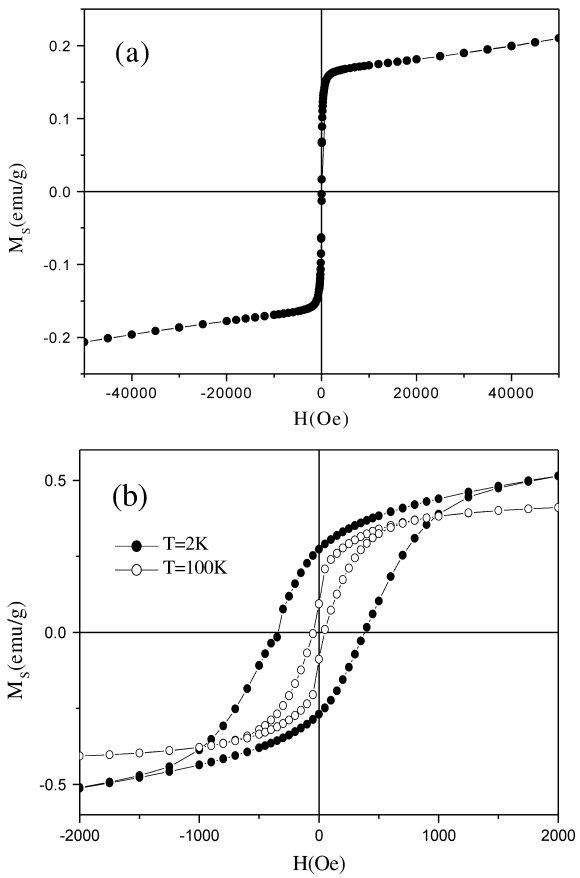

Fig. 4. Magnetic hysteresis loops of the Ni–AlMCM41 (H_2 reduction at 450 °C) measured at (a) 300, (b) 2 and 100 K.

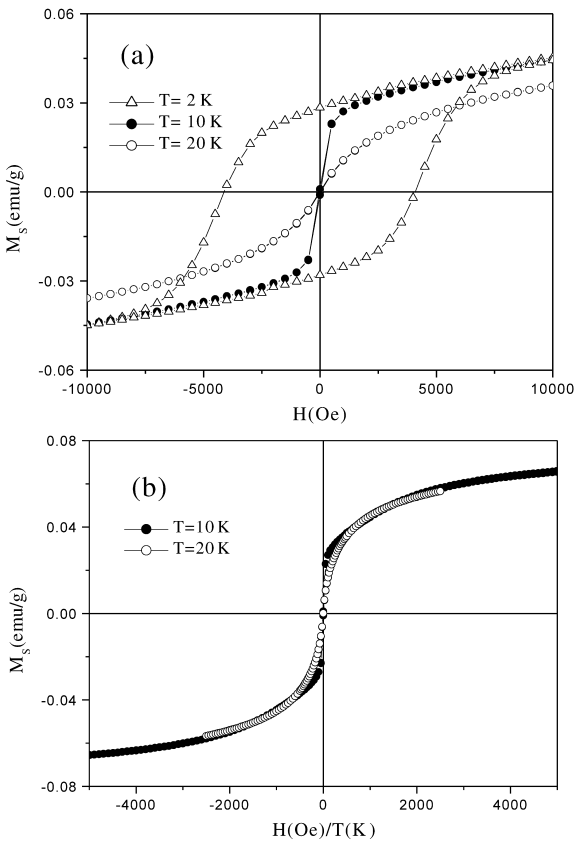

Fig. 5. Magnetic hysteresis loops of the Ni–AlMCM41 ($NaBH_4$ reduction) measured at (a) 2, 10, and 20 K, (b) H/T superposition.

the Langevin curve fitting is due to the difference between the actual anisotropy constant of Ni nanoparticles and the literature anisotropy data of bulk Ni.

In contrast to the size distribution observed in the solution method, a slightly broadened maximum pattern is shown in the inset of Fig. 3, which suggests a broader size distribution of the particles in the material is prepared by the solid reduction method. However, the particle size is considered to be not larger than the host pore from the non-existence of the Ni crystal peak in XRD and the large Ni particles in TEM pictures. It suggests that the particles exist not in a spherical form but in an elongated morphology.

4. Conclusions

Nanoparticles of nickel in an AlMCM41 have been synthesized by the H_2 reduction of Ni^{2+} in solid state and sodium borohydride reduction of Ni^{2+}–AlMCM41 in aqueous solution. The blocking temperature is different depending on reduction method [$T_b = 5$ K (solution method), $T_b = 240$ K (solid method)]. In contrast to the narrow size distribution of finely divided nickel metal particles in the solution method, larger and broader size distribution in the solid method.

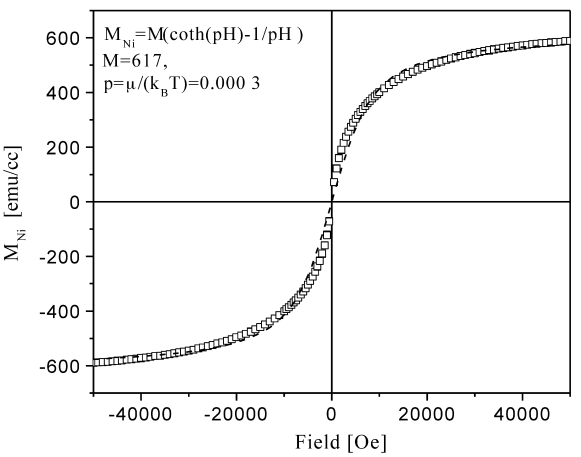

Fig. 6. Langevin function of Ni–AlMCM41 ($NaBH_4$ reduction) at 20 K.

Acknowledgments

This work was supported by Grant No. 1999-2-121-004-5 from the interdisciplinary research program of the KOSEF and by the US Department of Defense (DARPA Grant No. MDA972-97-1-0003) and also Konkuk University (J-H J).

References

[1] H. Sleiter, Prog. Mater. Sci. 33 (1989) 223.
[2] J. Shi, S. Gider, K. Bakcock, D.D. Awschalom, Science 271 (1996) 937.
[3] R.P. Andres, R.S. Averback, W.L. Brown, L.E. Brus, W.A. Goddard III, A. Kaldor, S.G. Louie, M. Moscovits, P.S. Peercy, S.J. Riley, R.W. Siegel, F. Spaepen, Y. Wang, J. Mater. Res. 4 (1989) 704.
[4] K.S. Suslick, S.B. Choe, A.A. Cichowlas, M.W. Grinstaff, Nature 353 (1991) 414.
[5] K.S. Suslick (Eds.), Ultrasound; Its Chemical, Physical and Biological Effects, VCH, Weinheim, Germany, 1988.
[6] S. Ramesh, Y. Kotypin, R. Prozorov, A. Gedanken, Chem. Mater. 9 (1997) 546.
[7] R.F. Ziolo, E.P. Giannelis, B.A. Weinstein, B.N. Ganguly, V. Mehrotra, M.W. Russel, D.R. Huffman, Science 257 (1992) 219.
[8] J.S. Beck, J.C. Vartuli, W.J. Roth, M.E. Leonowicz, C.J. Kresge, K.D. Schnitl, C.T.-W. Chu, K.H. Olson, E.W. Sheppard, S.B. McCullen, J.B. Higgins, J.L. Schlenken, J. Am. Chem. Soc. 114 (1992) 10834.
[9] K. Moller, T. Bein, Chem. Mater. 10 (1998) 2950.
[10] U. Ciesla, F. Schuth, Microporous Mesoporous Mater. 27 (1999) 131.
[11] J.-S. Jung, W.-S. Chae, R.A. MaIntyre, C.T. Seip, J.B. Wiley, C.J. O'Connor, Mater. Res. Bull. 34 (1999) 1353.
[12] G.N. Glavee, K.J. Klabunde, C.M. Sorensen, G.C. Hadjipanayis, Inorg. Chem. 32 (1993) 474.
[13] L. Zhang, A. Manthiram, J. Mater. Chem. 6 (1996) 999.
[14] C.J. O'Connor, Prog. Inorg. Chem. 29 (1982) 203.
[15] J.M. Kim, J.H. Kwak, S. Jun, R. Ryoo, J. Phys. Chem. 99 (1995) 16742.
[16] R. Ryoo, C.H. Ko, R.F. Howe, Chem. Mater. 9 (1997) 1607.
[17] K.J. Edler, J.W. White, Chem. Mater. 9 (1997) 1226.
[18] A. Chenite, Y.L. Page, A. Sayari, Chem. Mater. 7 (1995) 1015.
[19] C.P. Bean, J.D. Livingston, J. Appl. Phys. 30 (1959) 1205.
[20] J.L. Dormann, D. Fiorani, E. Tronc, Magnetic relaxation in fine particle systems, Adv. Chem. Phys. XCVIII (1997).
[21] D.L. Leslie-Pelecky, R.D. Rieke, Chem. Mater. 8 (1996) 1770.